Biointerphases
A Journal of Biomaterials and Biological Interfaces

Chemical physics of water–water interfaces

Mark Vis, Ben H. Erné, and Robert H. Tromp

Citation: Biointerphases **11**, 018904 (2016); doi: 10.1116/1.4939102
View online: http://dx.doi.org/10.1116/1.4939102
View Table of Contents: http://scitation.aip.org/content/avs/journal/bip/11/1?ver=pdfcov
Published by the AVS: Science & Technology of Materials, Interfaces, and Processing

Chemical physics of water–water interfaces

Mark Vis and Ben H. Erné
Van't Hoff Laboratory for Physical and Colloid Chemistry, Debye Institute for Nanomaterials Science, Utrecht University, Padualaan 8, 3584 CH Utrecht, The Netherlands

Robert H. Tromp[a)]
Van't Hoff Laboratory for Physical and Colloid Chemistry, Debye Institute for Nanomaterials Science, Utrecht University, Padualaan 8, 3584 CH Utrecht, The Netherlands and NIZO food research, Kernhemseweg 2, 6718 ZB Ede, The Netherlands

(Received 15 November 2015; accepted 16 December 2015; published 8 January 2016)

A brief review is given on recent progress in experimental and theoretical investigations of the interface between coexisting aqueous phases of biopolymers. The experimental aspects are introduced using results obtained from a model system consisting of aqueous mixtures of nongelling gelatin and dextran. The focus is on the interfacial tension and interfacial electric potential (Donnan potential). These quantities are experimentally accessible and can be shown to be closely related. © *2016 American Vacuum Society*. [http://dx.doi.org/10.1116/1.4939102]

I. INTRODUCTION

Due to the trend toward biodegradable products, low-calorie food, and sustainable ingredient sources, there is a demand for functionalizing fully water-based fluid systems. Such systems should have the same structure, appearance, rheology, mouth feel, or nutritional value as nonbiodegradable or high-caloric traditional analogs. Examples are paint, food emulsions such as mayonnaise, meat, and packing materials. In many of these cases, microscopic structure has to be generated and controlled with water as a continuous matrix. This structure is in some, often complicated, way related to phase separation between water and one or more ingredients, or between ingredients with water just acting as a dielectric, but otherwise inert matrix. This central role of structure formation, or in other words, phase stability in water-continuous mixtures, justifies a thorough study of the properties of the interfaces between phase regions that are formed by phase separation in aqueous solution of polymers. A detailed knowledge of these interfaces may be used, e.g., for stabilizing fully water-based emulsions, building structured water-based gels, and using water based emulsions as biocompatible carriers of pharmaceuticals.

Aqueous solutions containing chemically distinct polymers show phase separation above a certain concentration. The phase separation for such systems typically takes place above a few mass percent of each.[1–3] Temperature, salt concentration, *p*H, and molecular size may have a strong effect on this concentration. Salt will affect phase separation in the case of charged polymers by screening the repulsive interaction between charged polymers.[4] The effect of *p*H will be such that when polymers are more charged, they phase separate less easy. Larger molecular size will stimulate phase separation due to a reduction in mixing entropy.[5] Temperature has mainly an effect when it changes the solubility of polymers. For instance, when proteins unfold due to heat-induced denaturation, they become less soluble, and phase separation between water and protein will take place phase, increasing the effective molecular size and stimulating separation between protein and other polymers.[5,6] In the case of polysaccharides which are able to form helices, temperature-induced chain stiffness from helix formation will enhance phase separation from other polymers.[7,8] Both protein unfolding and helix formation will often lead to gelation of the particular compound. Gelation will arrest the fluid–fluid phase separation.[9,10] Although the gelled state is often very relevant for applications, no macroscopic interfaces are formed, which are accessible to experimental investigation. Therefore, the experimental data reviewed here are obtained from fluid phase separating solutions. For the sake of conciseness, only ternary mixtures (polymer A, polymer B, and water) will be considered, which show segregative phase separation, i.e., phase separation leading to two phases each enriched in one of the two polymers. The alternative, aggregative phase separation leading to two phases,[1,11] one of which is enriched in both polymers, will not be considered.

Many water soluble polymers of practical or industrial relevance show phase separation when their solutions are combined, such as casein, pectin, xanthan, modified cellulose, maltodextrin, modified starches, and nonfood grade polymers such as poly(ethylene oxide). In general, mixtures of proteins and polysaccharides tend to phase separate more readily than mixtures of different proteins or mixtures of different polysaccharides. This is due to the fact that an important driving force is the difference in water affinity. Systems that are in particular suitable for the study of water–water interfaces and emulsions do not gel, do not contain aggregates or complexes, and form clear phases. In that case, all turbidity can be ascribed to the existence of phase regions. Examples of systems which meet these conditions are gelatin/pullulan[12] gelatin/dextran,[13,14] and dextran/PEO.[15–18] The gelatin should be nongelling gelatin, e.g., gelatin from cold water fish. Most experimental examples in this review

[a)]Electronic mail: hans.tromp@nizo.com

are obtained from mixtures of nongelling gelatin and dextran.

Segregative phase separation will start by the formation of microstructure [e.g., droplets, Fig. 1(a)] in the spatial distribution of the two polymers, and eventually result in the formation of macroscopic phases. In the case of a density difference between the phases (the general case), the phases will be layers [see Fig. 1(b)]. Stirring, shaking, or some other form of shear will break up the phases, leading to a state which we will call a water-in-water emulsion, because they contain droplets of one aqueous phase, rich is one polymer, embedded in a continuous aqueous phase rich in the other polymer. It will be shown that the entropy of small ions, the counter ions of the charged polymers involved, and those ions from added low molar mass salt play a crucial role in the conditions needed for phase separation and the ensuing interfacial tension between the phase regions.

II. PHENOMENOLOGY OF WATER-IN-WATER EMULSIONS

The phase-separated state of solutions of polymers is characterized by a very low interfacial tension[17,19–24] typically 1 μN/m, i.e., a factor of 10^4 lower than the interfacial tension of oil–water interfaces. Therefore, even in the case of low viscosities of the phases, the rate of growth of phase regions, set by the ratio γ/η (γ is the interfacial tension and η is the viscosity), is slower by about the same factor. The progress of phase separation into macroscopic phase layers, such as in Fig. 1(a), is determined by the density difference between the phases, as well as the viscosities. This density difference is caused by the difference in water binding of the two polymers (and to a lesser extent by the difference in specific density of the polymers) and found[25] to be in the range of 1–10 g/l. For oil and water, the density difference is typically 100 g/l, so the achievement of full phase separation under gravity for water–water mixtures may take days instead of minutes to hours, as is the case for oil–water mixtures. In practice, when studying water–water interfaces, centrifugation is necessary to obtain pure phases without dispersed droplets of the other phase.

The density difference of coexistent aqueous phases is, as mentioned above, related to the difference in water content. It is therefore a subtle quantity, which can be easily manipulated by temperature and salt concentration. This is demonstrated in Fig. 1(c), where fully phase separated gelatin–dextran mixtures slightly differing in salt content show opposite relative densities of the phases. With increasing salt concentration, the gelatin-rich phase (wetting the glass wall) becomes less dense, crossing the density of the dextran-rich phase. This matching point is influenced by *p*H and temperature.

Due to the low interfacial tension, the structure of water-in-water emulsions is extremely sensitive to shear.[26,27] The shear, affecting the shape of a droplet, is expected to be comparable to the Laplace pressure inside the drop. With a

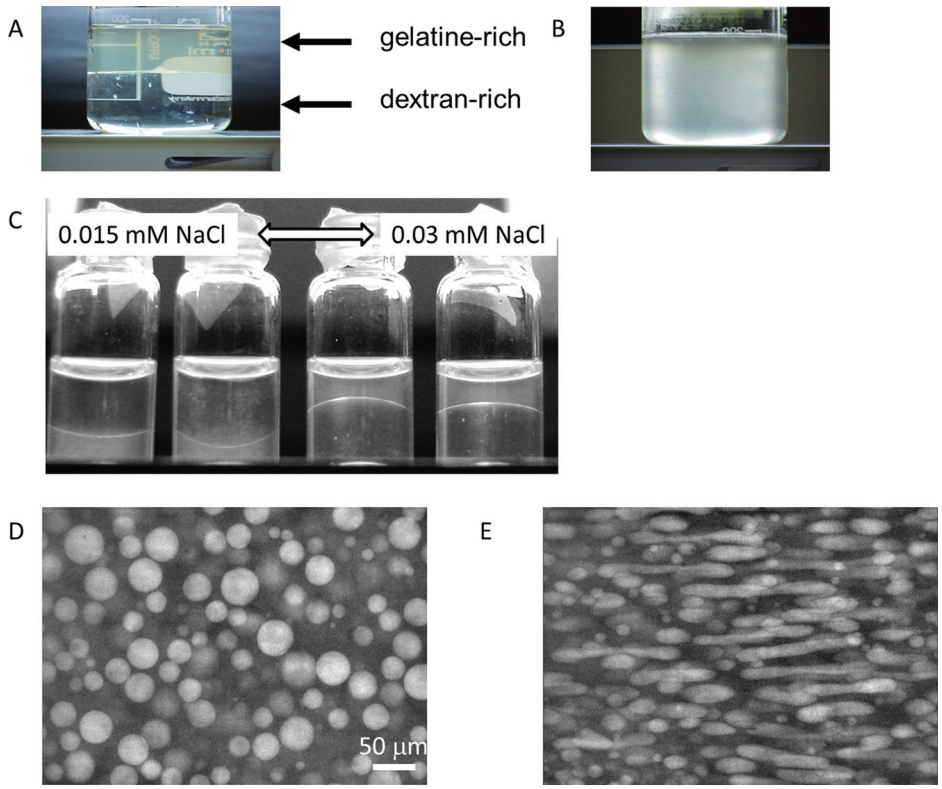

FIG. 1. Various appearances of aqueous phase-separated nongelling gelatin-dextran solutions of a concentration of 5%–10% of each polymer. (a) and (b) Macroscopic situation before and after break-up by stirring; (c) close up of a series of salt (NaCl) concentrations, giving rise to a density matching point; (d) and (e) microscopic views of the system in (a) and (b) after shear and during a shear rate of 7.5 s^{-1}.

droplet size of 20 μm [see Fig. 1(d)], this pressure is on the order of $2\gamma/R \approx 0.1$ Pa. The overall viscosities of the systems shown in Fig. 1 are on the order of 0.01 Pa s. Therefore, a shear rate on the order of $10\,s^{-1}$ is sufficient to deform the structure, as is demonstrated in Fig. 1(e). In general, the precise response of the structure to shear is not only set by the interfacial tension, but also by the viscosity ratio of the dispersed and continuous phases. At viscosity ratios far from one, and at phase volume ratios close one, shear and vorticity banding can be observed.

III. THEORETICAL BACKGROUND

The starting point for the theory of phase separation in solutions of two polymers (labeled A and B) and the calculation of the phase diagrams and interfacial tensions is usually the so called "blob" model,[28] which describes a ternary, semidilute (i.e., with a concentration c above the overlap concentration c^*) polymer solution as if it were a binary solution. This model assumes that the solvent quality is "good," which means that monomers try to avoid each other. As a consequence, the chains of segments take the conformation of a self-avoiding random walk. In the blob model, it is assumed that monomers interact only with other monomers that are close by. Therefore, by grouping interacting monomers in a single unit, called blob, the structure of the polymer is rescaled into a sequence of noninteracting blobs. The presence of solvent is now absorbed in the size of a blob. What is left is a binary mixture of ideal polymers of blobs. The mean field approximation (when the size of compositional fluctuations in the mixed state and the interfacial width in the demixed state are not much larger than a blob size, i.e., far from the critical point of mixing) of the free energy of mixing F can now be expressed by the Flory–Huggins equation,[5] rescaled on the blob size[29]

$$\frac{F}{Vk_BT} = \frac{1}{\xi(c)^3}\left[\frac{\varphi}{N_b(c)}\log\varphi + \frac{1-\varphi}{N_b(c)}\log(1-\varphi) + u(c)\varphi(1-\varphi) + K\right], \tag{1}$$

with the blob size

$$\xi(c) = 0.43R_g\left(\frac{c}{c^*}\right)^{\frac{\nu}{1-3\nu}}, \tag{2}$$

the number of blobs per chain

$$N_b(c) = \frac{N}{\xi(c)^3 c}, \tag{3}$$

and the dimensionless interaction strength

$$u(c) = u_{\mathrm{crit}}\left(\frac{c}{c_{\mathrm{crit}}}\right)^{\frac{\gamma}{3\nu-1}} = \frac{2}{N_{b,\mathrm{crit}}}\left(\frac{c}{c_{\mathrm{crit}}}\right)^{\frac{\gamma}{3\nu-1}}, \tag{4}$$

(T is the absolute temperature, V is the volume, k_B is Boltzmann's constant, φ is the volume fraction of blobs of polymer A, R_g the radius of gyration of the polymers in dilute, nonoverlapping conditions, N the number of monomers per chain, and u_{crit} the interaction strength at the critical concentration c_{crit}). The solvent quality of water for both polymers is assumed to be good, so $\nu = 3/5$, and $\chi \approx 0.22$.[30] $K \approx 0.024$ represents the contribution from the excluded volume interaction between monomers inside a blob and is independent of the type of polymer for a good solvent.[30] R_g and N are taken to be the same for polymers A and B. It should be noted that the factor of 0.43 in Eq. (2) needs careful experimental verification, for instance, by light scattering, as it has a strong effect on calculated values of experimentally accessible properties such as interfacial tension.[30]

For polymers A and B with unequal values of N, Eq. (1) can be shown to transform to[31]

$$\frac{F}{Vk_BT} = \frac{\varphi}{N_{b,A}\xi_A^3}\log\varphi + \frac{1-\varphi}{N_{b,B}\xi_B^3}\log(1-\varphi) + \frac{\omega}{\xi_{eff}^3}\varphi(1-\varphi) + \frac{K}{\xi_{eff}^3}, \tag{5}$$

with the dimensionless interaction parameter

$$\omega = \frac{\left(1+\sqrt{\alpha}\right)^2}{(1+\alpha)}\left(\frac{c}{c_{\mathrm{crit}}}\right)^{\frac{-\chi-1}{1-3\nu}}, \tag{6}$$

($\alpha = N_A/N_B$, the ratio of the degrees of the numbers of monomers per chain and ${\xi_{eff}}^{-1} = ({\xi_A}^{-1} + {\xi_B}^{-1})/2$). From Eq. (1) or (5), the phase diagram of mixing can be calculated by the standard procedure of equating the pressures and chemical potentials of the coexisting phases.

In the case of one or both of the polymers being charged, there will, in general, be an unequal distribution of small ions between the phases. This inhomogeneous distribution of ions corresponds to a lowering of the ion entropy relative to that in the mixed state. Polymer charge therefore causes the free energy of mixing to increase and the tendency to phase separation to be suppressed.[3] The simplest case to study is a mixture of a charged and a noncharged polymer. Only when the charged polymer is weakly charged, or in the presence of a high salt concentration, phase separation will take place. Full expressions for the change in ion entropy upon phase separation can be found in Ref. 32. An approximation for the case in which the concentration of salt is larger than the concentration of counter ions, a very common practical situation, is

$$\frac{\Delta S_{\mathrm{ion}}}{Vk_b} \approx -\frac{1}{2}\theta(1-\theta)\frac{z^2(c_1-c_2)^2}{2c_s + z\left[c_1\theta + c_2(1-\theta)\right]}, \tag{7}$$

where θ is the volume fraction of phase 1 in the total volume, c_i is the concentration of charged polymer in

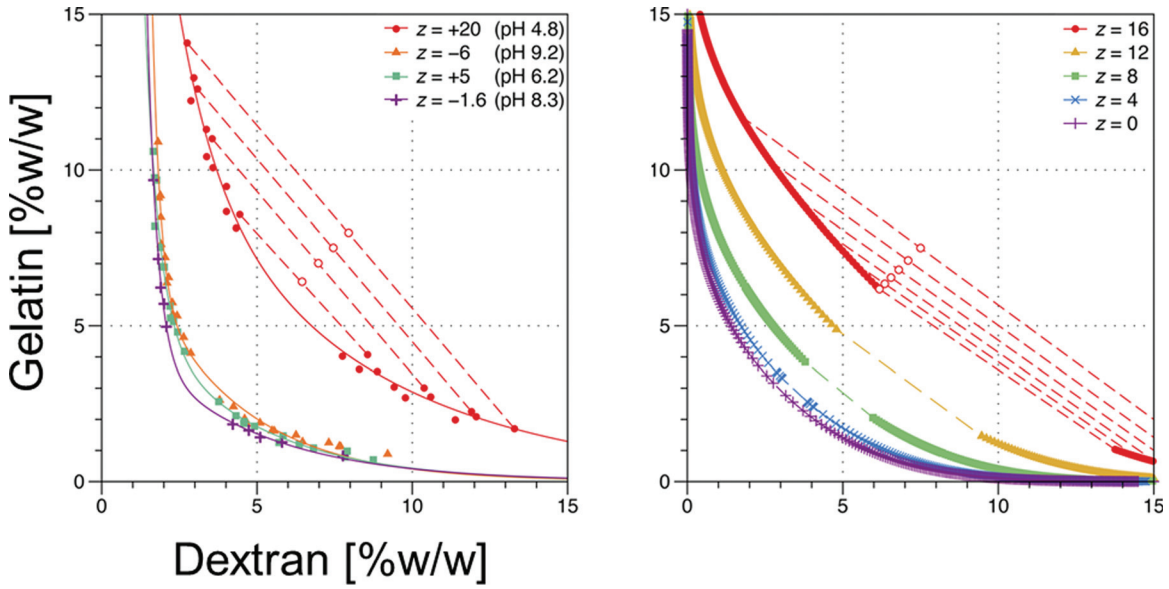

FIG. 2. Representative phase diagrams of mixing (Ref. 32); experimental (left) and calculated using the free energy of mixing [Eq. (1)] combined with small ion entropy [Eq. (7)]. Reprinted with permission from Vis *et al.*, Macromolecules **48**, 2819 (2015). Copyright 2015 American Chemical Society.

phase i, c_s is the overall salt concentration, and z in the number of charges per chain of the charged polymer. When all small ions are from added salt, there is no charged polymer, and no effect from phase separation on the small ion entropy. Some experimental and calculated phase diagrams are shown in Fig. 2. For the calculations, Eq. (1) was supplemented with the small ion entropy approximated by Eq. (7). It may be noted that in the binodals in the experimental phase diagram do no approach a zero gelatin concentration at overall concentrations. This effect stems from the polydispersity of the polymers used. The low molar mass fraction does not fully take part in the phase separation, giving rise to a significant concentration of (in this case) dextran in the gelatin-rich phase. It turns out that the dextran-rich phase contains much less gelatin at high overall concentration.

When in spite of its unfavorable effect on small ion entropy phase separation takes place, the charged polymer as well as its associated counter ions is to a given extent confined into one phase. However, due to their vastly different entropies, the counter ions are much less confined than the charged polymers. This difference gives rise to an electric potential difference between the phases, the well-known Donnan potential,[33] commonly found across semipermeable membranes, of which as water–water interfaces are an example. An expression for the Donnan potential in the presence of sufficient salt can be derived from similar considerations as for Eq. (7)

$$\psi_D \cong \frac{k_B T}{e} \frac{z(c_1 - c_2)}{2c_s}, \tag{8}$$

(e is the elementary charge). The Donnan potential arises due to the need for local charge neutrality in the bulk of the phases and the difference in concentration of the charged polymer. This leads to a difference in the concentration of small ions in the two phases. In the compositional profiles across the interface, local charge neutrality has to be violated resulting in the electric potential difference. Figure 3 shows some experimental data[34] for the interface between the coexisting dextran- and gelatin-rich phases. The further the *p*H is from the isoelectric point of gelatin (*p*H 7–8), the higher the absolute value of the Donnan potential. At the isoelectric point, the Donnan potential changes sign.

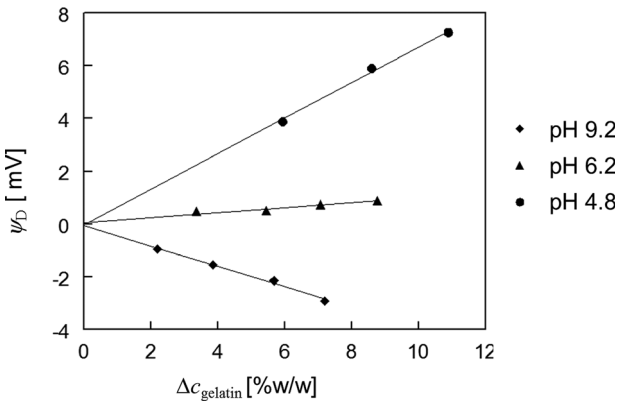

FIG. 3. Measurements of the Donnan potential for some *p*H values as a function of the difference in the mass fraction of gelatin in the two phases. Below the isoelectric point (app. *p*H 7.5), a positive, and at higher *p*H a negative potential is found. The lines are linear fits through the origin, according to Eq. (8). Adapted with permission from Vis *et al.*, Langmuir **30**, 5755 (2014). Copyright 2014 American Chemical Society.

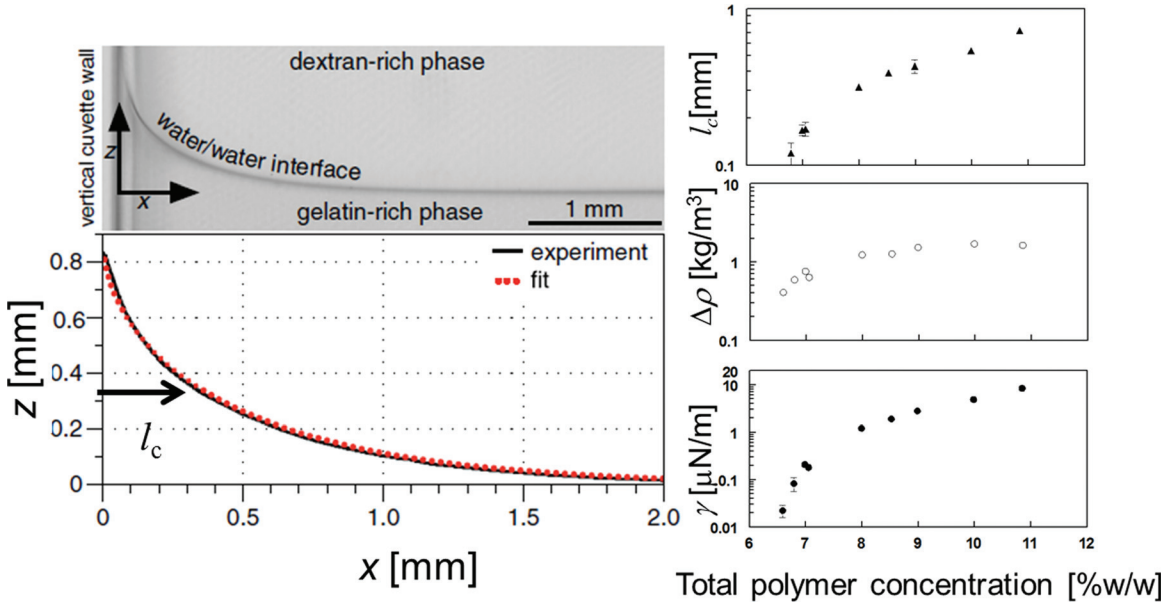

FIG. 4. Mensicus and the measurement of the corresponding capillary length of coexisting aqueous phases of dextran and nongelling gelatin (left), and representative experimental results of the capillary length l_c, density differences between the phases and resulting interfacial tension. Adapted from Vis *et al.*, Macromolecules **48**, 7335 (2015).

IV. INTERFACIAL TENSION

A. Experiment

The interfacial tension of water–water interfaces can be measured by the spinning drop method[20,35,36] by interfacial deformation using a laser beam,[37] from relaxation of shear[23,38] or by recording the shape of the meniscus in equilibrium.[25,39,40] The latter was found to give the most reliable results and is therefore illustrated here (Fig. 4). In a cuvette, full phase separation is allowed to take place under gravity or centrifugation. The resulting shape of the meniscus can be described by an analytical solution of the force balance between Laplace pressure, gravitation, and wetting of the wall.[40] The fit of this solution to the experimental shape gives the capillary length $l_c = \sqrt{\gamma/g\Delta\rho}$. When the density difference $\Delta\rho$ is known, the interfacial tension can be calculated. Figure 4 also gives representative experimental results, from which it can be concluded that the interfacial tension can be measured in this way over 3 orders of magnitude (from 0.01 to 10 μN/m).

B. Theory

1. Uncharged systems

The interfacial tension, γ, and the interfacial width, d, can be roughly estimated[29] from the adjusted expression by Helfand and Tagami[41] for infinite degree of polymerization in blends

$$\gamma = \frac{k_B T}{b^2}\sqrt{\frac{\chi_{AB}\varphi}{6}}, \tag{9}$$

and

$$d = \frac{b}{\sqrt{6\chi_{AB}\varphi}}, \tag{10}$$

with φ the volume fraction of polymer in the solution and χ_{AB} the interaction parameter from the Flory–Huggins equation for blends

$$\frac{F}{Vk_BT} = \frac{\phi}{N_A}\log\varphi + \frac{1-\phi}{N_B}\log(1-\phi) + \chi_{AB}\varphi(1-\phi), \tag{11}$$

where ϕ is the volume fraction of polymer A in the blend. This approach amounts to assuming that the interaction parameter decreases proportionally to the "dilution" by solvent. The excluded volume corresponding to the local repulsion of chain segments is in that case ignored. χ_{AB} is of the order of 10^{-2}–10^{-3} and $b \approx 1$ nm, so $\gamma \approx 6$–50 μN/m for $\varphi = 0.1$. The experimental value is usually lower, because the degree of polymerization is finite, and because the presence of solvent in the system imparts compressibility, which allows the system to weaken the gradient at the interface by absorbing excess solvent at the interface. In order to account for the finite degree of polymerization, excluded volume and compressibility, the expression for the interfacial tension in a phase separated binary blend, i.e., the excess free energy due to the presence of an interface

$$\frac{F_{ex}}{Ak_BT} = \frac{1}{b^3}\int_V dz\left[\frac{\varphi}{N}\log\varphi + \frac{1-\varphi}{N}\log(1-\varphi) + \chi\varphi(1-\varphi) + b^2\frac{|\nabla\varphi|^2}{24\varphi(1-\varphi)}\right] \tag{12}$$

is modified by using Eq. (1) for the free energy of mixing, and allowing for gradients not only in composition, but also in the total concentration c of polymer:[29]

$$\frac{\Omega_{ex}}{Ak_BT} = \int_V dz \left[\begin{array}{l} \frac{\varphi}{N_b\xi^3}\log\varphi + \frac{1-\varphi}{N_b\xi^3}\log(1-\varphi) + \frac{u}{\xi^3}\varphi(1-\varphi) \\ \quad + \frac{K}{\xi^3} + \frac{|\dot{\eta}|^2}{24\xi(1-\eta^2)} + \frac{\bar{u}^2|\dot{\varepsilon}|^2}{24\xi(1-\bar{u}\varepsilon)^2} - \mu_\eta\eta - \mu_\varepsilon\varepsilon + \bar{p} \end{array} \right], \quad (13)$$

(in which $\eta(z) \equiv 2\varphi(z) - 1$, and $\varepsilon(z) \equiv [c(z) - \bar{c}]/\bar{u}\bar{c}$ derivatives to z are indicated by a dot and bulk values, far from the interface, are indicated by a bar). Use of the grand potential $\Omega_{ex} = F_{ex} - \mu_\eta\eta - \mu_\varepsilon\varepsilon + pV$ is convenient because the composition of the interface is not fixed. Instead, it is determined by the chemical potential of the solvent in the bulk. When the gradients of composition and concentration are assumed to be uncoupled (exact in symmetrical cases) and the solvent concentration at the interface is only slightly lower than in the bulk (i.e., $\bar{u}\varepsilon(0) \ll 1$), it can be shown that the interfacial tension can be expressed as the sum of three terms (details of this calculation can be found in Refs. 29 and 31)

$$\gamma = \gamma_\infty(1 - \Delta_1 - \bar{u}\Delta_2) = \frac{k_BT}{\bar{\xi}^2}\sqrt{\frac{\bar{u}}{6}}(1 - \Delta_1 - \bar{u}\Delta_2), \quad (14)$$

with

$$\Delta_1 = 1 - \int_0^{\bar{\eta}} d\eta \frac{\dot{\eta}(x)}{1-\eta^2}, \quad (15)$$

and

$$\Delta_2 = -\frac{1}{8}\int_{-\infty}^{\infty} dx \left[\frac{-\dot{\eta}(x)^2}{(1-\eta^2)} + \frac{1+\chi}{(3\nu-1)}(\eta^2 - \bar{\eta}^2)\right]\varepsilon(x). \quad (16)$$

Δ_1 accounts for the finite degree of polymerization, which facilitates interpenetration of the phases and weakening of the interfacial compositional gradient. Δ_2 accounts for the lower polymer concentration at the interface, which also weakens the interfacial gradient. Δ_2 is predicted to lower the interfacial tension by as much as 20% relative to the (fictional) case in which the solvent concentration is unaffected by the presence of the compositional gradient. Quantitative verification is however not yet available. Such a verification could be carried out by choosing a pair of noncharged monodisperse phase separating polymers with equal degrees of polymerization and Kuhn's lengths. The latter is necessary because different values of N or b could lead to a preferential curvature of the interfaces which are expected to have a small effect on the interfacial tension.[31] Monodispersity is necessary because the low molar mass fraction may not fully take part in the phase separation. Moreover, the factor between the radius of gyration in dilute solution and the correlation length above the overlap concentration should be carefully measured by light scattering. For a pair of properly characterized, monodisperse polymers, the measured interfacial tension should be consistently lower than a prediction which ignores Δ_2.

2. Charged systems

From Fig. 2, a strong effect of the charge density of the charged polymer is concluded. This effect is much larger than the effect of changing the degree of polymerization within an experimentally useful range (results not shown). Therefore, polymer charge (modified by added salt) appears to be the most important variable in the phase separation behavior of a pair of polymers, one of which is charged.

The polymer charge enters the free energy of mixing by way of ion entropy, expressed by Eq. (7) and the separation of counter ions and charged polymers (i.e., positive and negative charges) at the interface. The latter gives rise to an interfacial electric potential. The combination of an interfacial electric potential balanced by entropic counter ions corresponds to an electric double layer. The free energy of an electric double layer is negative[42] (relative to the case of undissociated counter ions) and lowers therefore the interfacial tension of a water–water interface. This negative contribution to the interfacial tension is a function of the interfacial potential and the Debye screening length κ, and can be expressed by

$$\Delta\gamma \cong -\frac{k_BT\kappa}{16\pi\lambda_B}\Psi_D{}^2, \quad (17)$$

where λ_B is the Bjerrum length $= e^2/4\pi\varepsilon_0\varepsilon_r k_BT$ and $\Psi_D = e\psi_D/k_BT$ the dimensionless Donnan potential.

The effect of interfacial charge on the interfacial tension[25] is shown in Fig. 5. For an objective comparison between systems of different charge densities, the values of interfacial tensions should be taken at equal tie-line lengths, because only in that case the distance to the critical point of mixing, i.e., the "degree of phase separation" is the same. It turns out that for different charge densities of the charged polymer (gelatin), the interfacial tensions differ by about a factor of three. This difference, however, can be fully compensated for by taking into account that there is a difference in interfacial electric potential, calculated Eq. (17).

V. CONCLUSION AND FURTHER WORK

The interfacial tension of water–water interfaces has been explored experimentally, as a function of concentration and polymer charge. The contribution of charge can be accounted for in a quantitative way. The bare interfacial tension, however, has not yet been interpreted in terms of the

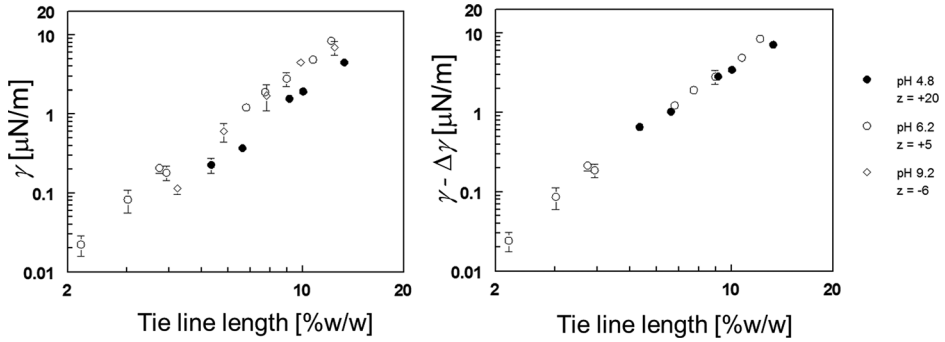

FIG. 5. Comparison of interfacial tensions as a function of the tie-line length (i.e., the difference in composition of the phases) without (left) and with (right) correction for the effect of interfacial charge.

shape of the concentration profile, which might be affected by the presence of a solvent gradient. For the latter, measurements of the profile are necessary. These are not yet available, but may be provided by neutron reflectometry.

A considerable amount of experimental data[43–47] is currently emerging in the area of manipulation of the water–water interface, with the aim to stabilize water-in-water emulsions. It has been shown that particles, in particular, polystyrene particles[43] or inorganic particles such as clay,[44] adsorb at the water–water interface. In some cases, stability is seen due to the Pickering effect. Another approach is by way of interface gelation or interface coacervation, by which the stability originates from an increase in interfacial viscosity due to a higher polymer concentration at the interface. A major hurdle in stabilizing water-in-water emulsions is the fact that the conditions for adsorption at the water–-water interface of molecules or particles remain unclear, although in general interface active compounds are expected to be marginally soluble in water, suggesting high molar masses for polymers or relative hydrophobicity for particles as first guesses for promising characteristics. When exploring particle adsorption at water–water interfaces, issues to be addressed are the influence of the ubiquitous polymer adsorption on the surface of the particles, interfacial crowding of particles giving rise to depletion interactions or interfacial aggregation, and the interaction between particle charge and interfacial Donnan potentials. These issues may be the focus of further research on water–water interfaces.

[1]J. T. G. Overbeek and M. J. Voorn, J. Cell. Comp. Physiol. **49**, 7 (1957).
[2]V. Y. Grinberg and V. B. Tolstoguzov, Food Hydrocolloids **11**, 145 (1997).
[3]I. Michaeli, J. T. G. Overbeek, and M. J. Voorn, J. Polym. Sci. **23**, 443 (1957).
[4]K. Bergfeldt, L. Piculell, and F. Tjerneld, Macromolecules **28**, 3360 (1995).
[5]P. F. Flory, *Principles of Polymer Chemistry* (Cornell University, Ithaca, NY, 1953).
[6]R. L. Scott, J. Chem. Phys. **17**, 279 (1949).
[7]R. P. Sear and G. Jackson, J. Chem. Phys. **103**, 8684 (1995).
[8]N. Loren *et al.*, Macromolecules **34**, 289 (2001).
[9]F. Sciortino, R. Bansil, H. E. Stanley, and P. Alström, Phys. Rev. E **47**, 4615 (1993).
[10]R. H. Tromp and R. A. L. Jones, Macromolecules **29**, 8109 (1996).
[11]J. van der Gucht, E. Spruijt, M. Lemmers, and M. A. Cohen Stuart, J. Colloid Interface Sci. **361**, 407 (2011).
[12]P. Ding, A. W. Pacek, W. J. Frith, I. T. Norton, and B. Wolf, Food Hydrocolloids **19**, 567 (2005).
[13]V. B. Tolstoguzov, V. P. Belkina, V. J. Gulov, V. J. Grinberg, E. F. Titova, and E. M. Belavzev, Stärke **26**, 130 (1974).
[14]R. H. Tromp, A. R. Rennie, and R. A. L. Jones, Macromolecules **28**, 4129 (1995).
[15]G. Johansson and H. Walter, Int. Rev. Cytol. **192**, 33 (2000).
[16]H. O. Johansson, G. Karlström, F. Tjerneld, and C. A. Haynes, J. Chromatogr. B **711**, 3 (1998).
[17]D. Forciniti, C. K. Hall, and M. R. Kula, Fluid Phase Equilibr. **61**, 243 (1991).
[18]M. W. Edelman, E. van der Linden, and R. H. Tromp, Macromolecules **36**, 7783 (2003).
[19]L. de Ruiter and H. G. Bungenberg de Jong, Proc. Kon. Acad. Wetensch. **50**, 836 (1947).
[20]E. Scholten, R. Tuinier, R. H. Tromp, and H. N. W. Lekkerkerker, Langmuir **18**, 2234 (2002).
[21]M. Simeone, A. Alfani, and S. Guido, Food Hydrocolloids **18**, 463 (2004).
[22]J. Ryden and P.-A. Albertsson, J. Colloid Interface Sci. **37**, 219 (1971).
[23]P. van Puyvelde, Y. A. Antonov, and P. Moldenaers, Food Hydrocolloids **16**, 395 (2002).
[24]Y. A. Antonov, P. van Puyvelde, and P. Moldenaers, Int. J. Biol. Macromol. **34**, 29 (2004).
[25]M. Vis, V. F. D. Peters, E. M. Blokhuis, H. N. W. Lekkerkerker, B. H. Erné, and R. H. Tromp, Macromolecules **48**, 7335 (2015).
[26]R. H. Tromp and E. H. A. de Hoog, Phys. Rev. E **77**, 031503 (2008).
[27]S. Caserta, L. Sabetta, M. Simeone, and S. Guido, Chem. Eng. Sci. **60**, 1019 (2005).
[28]P. G. de Gennes, *Scaling Concepts in Polymer Physics* (Cornell University, Ithaca, NY, 1979).
[29]D. Broseta, L. Leibler, O. Kaddour, and C. Strazielle, J. Chem. Phys. **87**, 7248 (1987).
[30]D. Broseta, L. Leibler, and J. F. Joanny, Macromolecules **20**, 1935 (1987).
[31]R. H. Tromp and E. M. Blokhuis, Macromolecules **46**, 3639 (2013).
[32]M. Vis, V. F. D. Peters, B. H. Erné, and R. H. Tromp, Macromolecules **48**, 2819 (2015).
[33]F. G. Donnan and Z. Elktrochem, Angew. Phys. Chem. **17**, 572 (1911).
[34]M. Vis, V. F. D. Peters, R. H. Tromp, and B. H. Erné, Langmuir **30**, 5755 (2014).
[35]B. Vonnegut, Rev. Sci. Instrum. **13**, 6 (1942).
[36]E. H. A. de Hoog and H. N. W. Lekkerkerker, J. Phys. Chem. B **105**, 11636 (2001).
[37]S. Mitani and K. Sakai, Phys. Rev. E **66** 031604 (2002).
[38]S. Tomotika, Proc. R. Soc. London Ser. A **150**, 322 (1935).
[39]D. G. A. L. Aarts, J. H. van der Wiel, and H. N. W. Lekkerkerker, J. Phys.: Condens. Matter **15**, S245 (2003).

[40]G. K. Batchelor, *An Introduction to Fluid Dynamics* (Cambridge University, Cambridge, 2002).
[41]E. Helfand and Y. Tagami, J. Chem. Phys. **56**, 3592 (1972).
[42]E. J. W. Verwey and J. T. G. Overbeek, *Theory of The Stability of Lyotropic Colloids* (Dover, Mineola, NY,1999).
[43]G. Balakrishnan, T. Nicolai, L. Benyahia, and D. Durand, Langmuir **28**, 5921 (2012).
[44]M. Vis, J. Opdam, I. S. J. van't Oor, G. Soligno, R. van Roij, R. H. Tromp, and B. H. Erné, ACS Macro Lett. **4**, 965 (2015).
[45]H. Firoozmand, B. S. Murray, and E. Dickinson, Langmuir **25**, 1300 (2009).
[46]A. T. Poortinga, Langmuir **24**, 1644 (2008).
[47]D. M. A. Buzza, P. D. I. Fletcher, T. K. Georgiou, and N. Ghasdian, Langmuir **29**, 14804 (2013).